nature cell biology

DOI: 10.1038/ncb1907

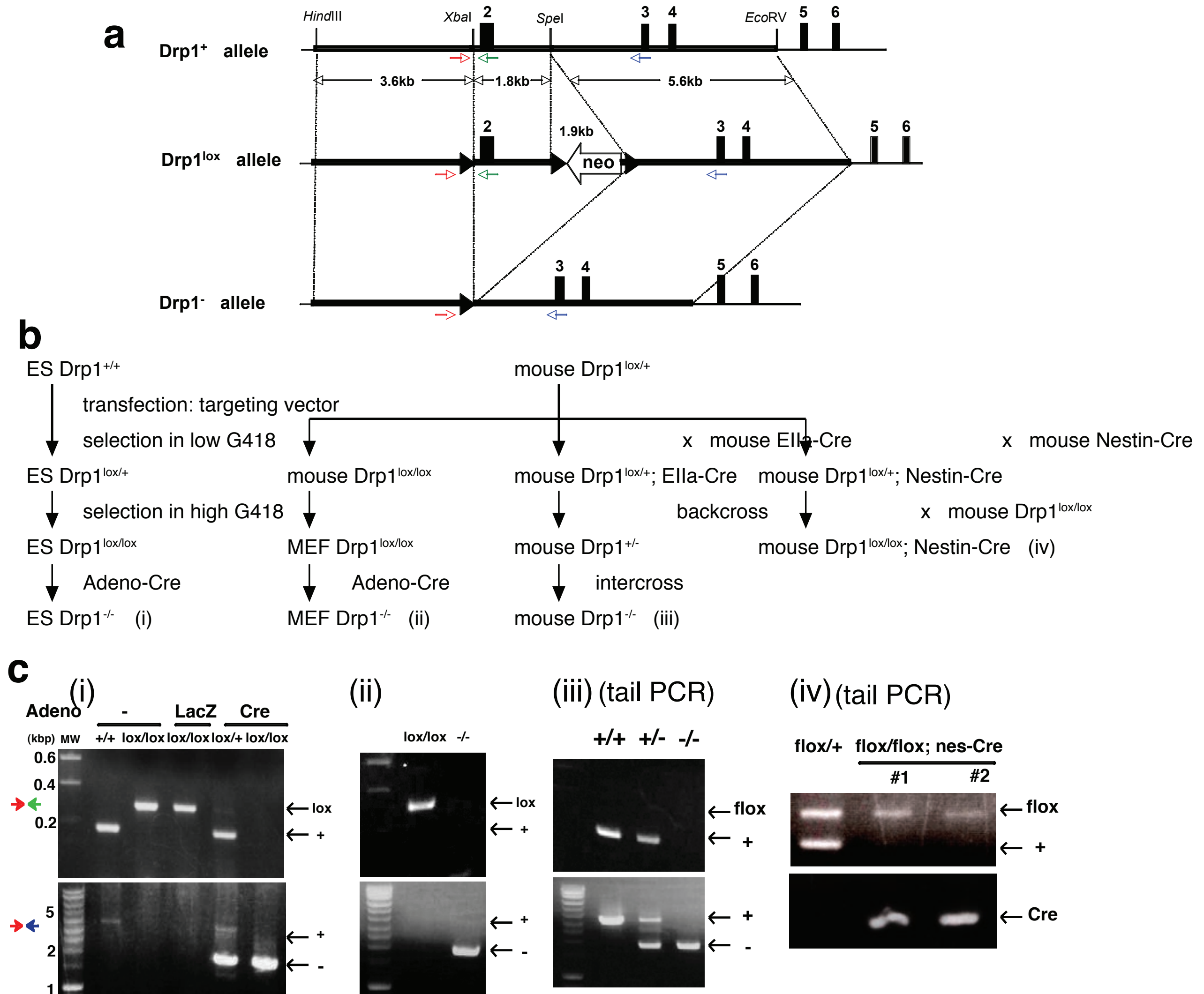

Figure S1 Generation of Drp1$^{-/-}$ cells and mice. **a**, Map of Drp1-targeting constructs. Wild-type Drp1 locus (Drp1^{+}), targeted Drp1 locus (Drp1^{lox}), and knockout Drp1 locus (Drp1^{-}). The arrowheads indicate the loxP sequence. The arrows indicate primers used for genotyping by PCR. **b**, Schematic diagram of constructions. **c**, Identification of floxed, or targeted Drp1 by PCR genotyping.

© 2009 Macmillan Publishers Limited. All rights reserved.

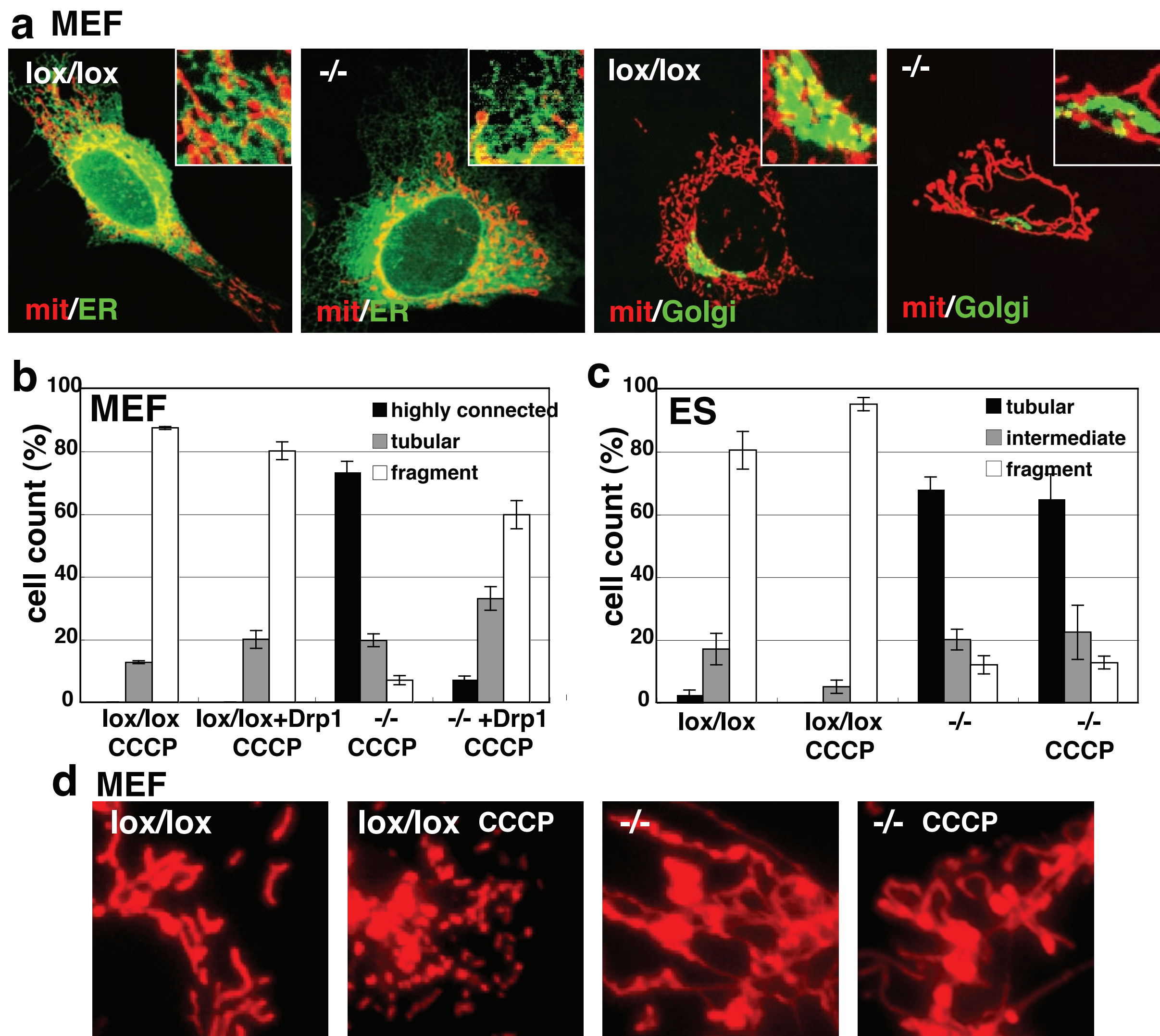

Figure S2 a, Morphology of the endoplasmic reticulum (GFP-cytochrome b5) and Golgi (YFP-Golgi) in controls and Drp1$^{-/-}$ MEFs was analyzed by fluorescence microscopy. Mitochondria (mit) were visualized by su9-RFP. **b** and **c**, MEFs and ES cells that had been transfected with or without the expression vector for rat Drp1 were treated with or without 20 μM CCCP for 2 h, then mitochondrial morphology was analyzed as in (**a**). Mitochondria with the indicated morphology in CCCP-treated or untreated MEFs and ES cells were quantified. At least 100 cells in 3 distinct fields were analyzed. **d,** Representative images in (**b**) are shown.

© 2009 Macmillan Publishers Limited. All rights reserved.

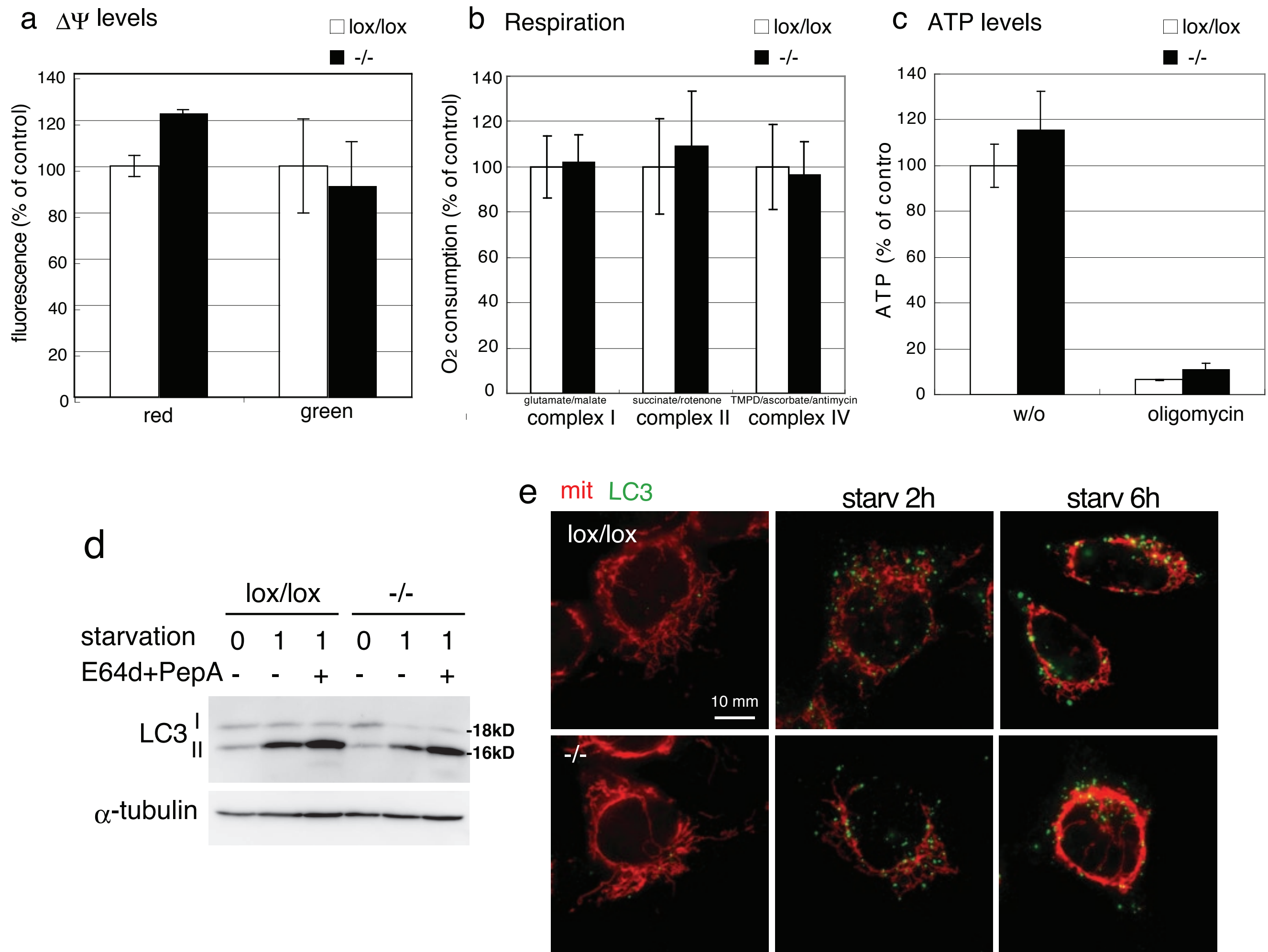

Figure S3 a, Analysis of the Ψ levels across the mitochondrial inner membrane. Control and Drp1$^{-/-}$ MEFs were cultured in the presence of 20 nM MitoTracker Red or 100 nM MitoTracker Green for 1 h. The fluorescent signal in each cell was counted for more than 100 cells in 3 distinct optical fields. **b**, Respiration of MEFs through complex I, II and IV. The harvested cells were incubated with the indicated respiratory substrates, and O2 consumption was measured using oxygen electrode. **c**, MEFs were incubated with or without 10 μM oligomycin for 10h and the cell extracts were subjected to ATP concentration analysis using luciferase. **d**, Wild-type and Drp1$^{-/-}$ MEFs were cultured in amino acids- and serum-depleted medium for 1 h in the presence or absence of lysosomal protease inhibitors (E64d + Pepstatin A). The cell lysates were subjected to SDS-PAGE and subsequent immunoblotting using the antibodies against LC3 and a-tubulin. **e**, Wild-type and Drp1$^{-/-}$ MEFs were cultured as in (**d**) for the indicated time periods, incubated with the antibodies against LC3 and Tom70, and analyzed by immunofluorescence microscopy.

© 2009 Macmillan Publishers Limited. All rights reserved.

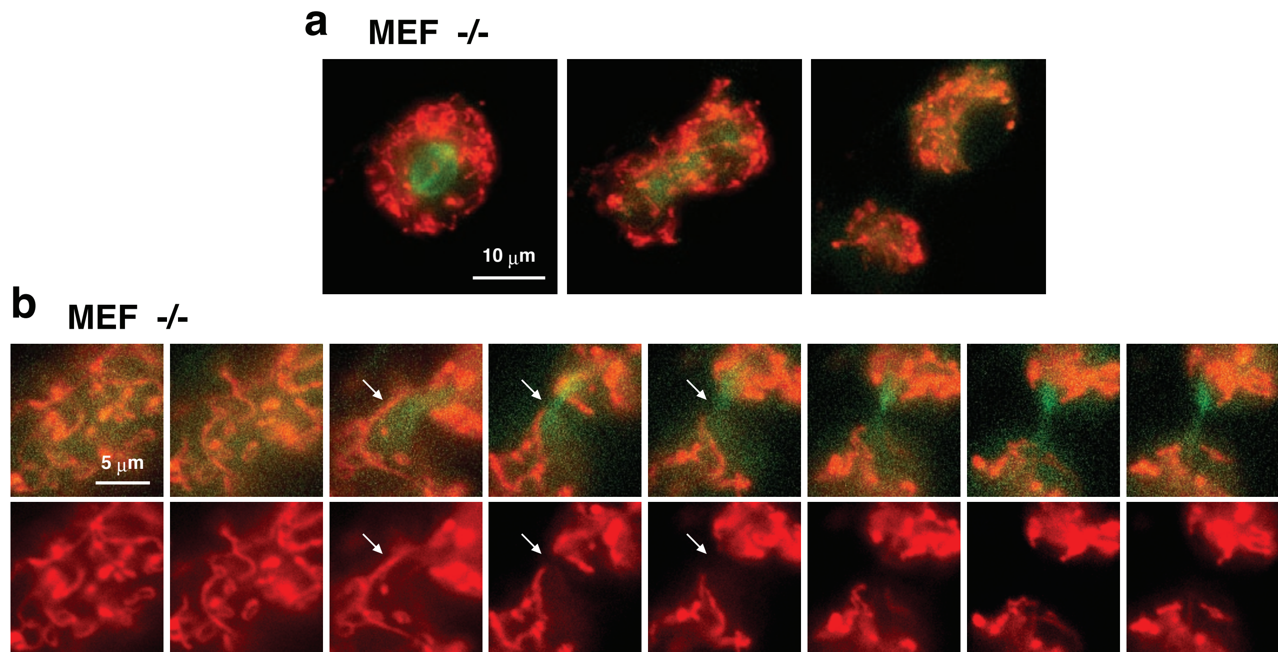

Figure S4 Time-lapse imaging of mitotic Drp1$^{-/-}$ MEFs expressing su9-RFP and YFP-α-tubulin. **b**, Mitochondria and a mitotic spindle in living cells were observed by fluorescence video microscopy for 1 h at 37°C at 2-min intervals. **a**, Representative images from (**b**) were depicted.

© 2009 Macmillan Publishers Limited. All rights reserved.

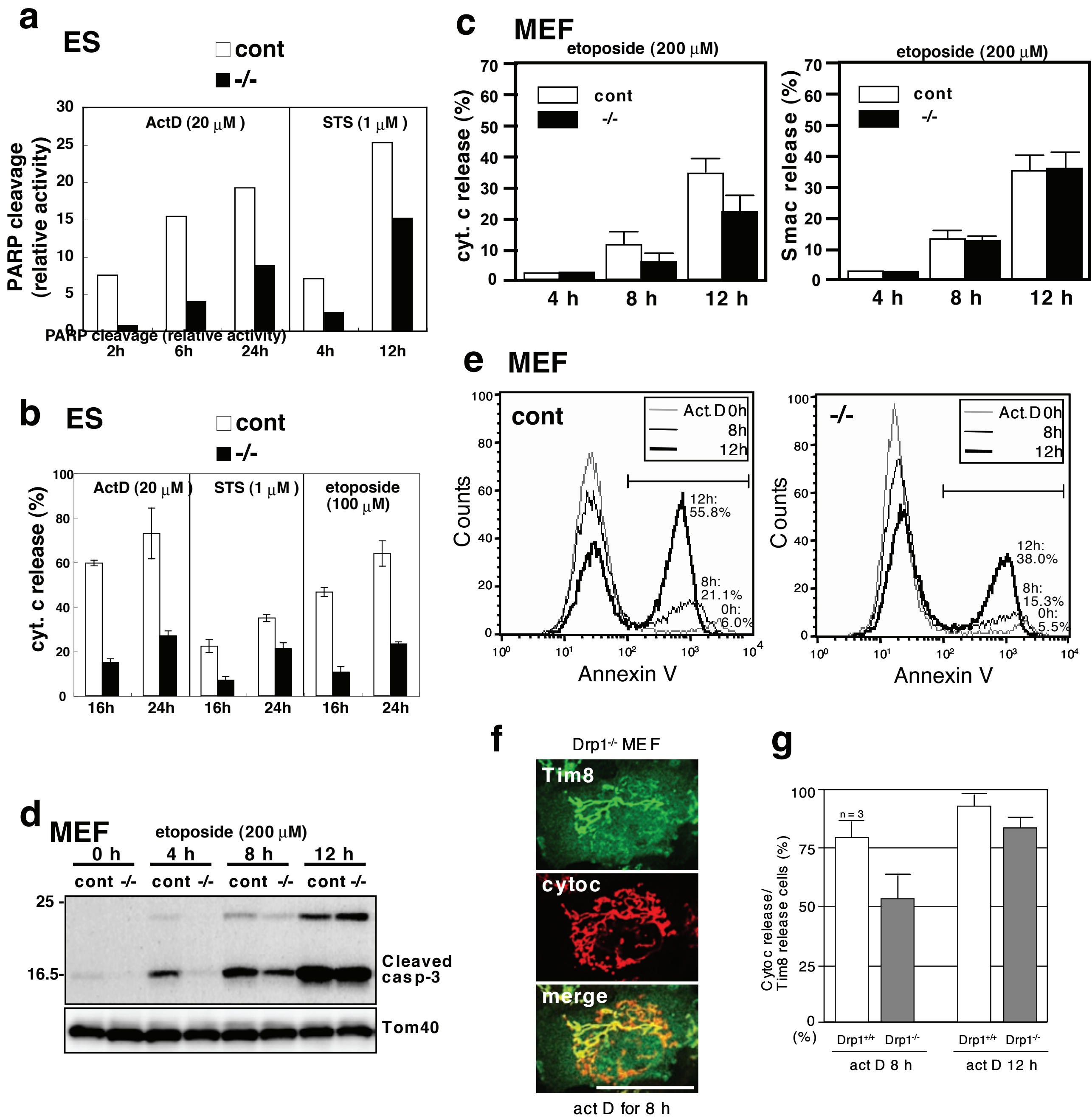

Figure S5 Response of Drp1$^{-/-}$ ES cells and MEFs to proapoptotic reagents. **a**, ES cells were treated with 1 μM staurosporine (STS) or 20 μM actinomycin D (ActD) and the processed PARP was quantified by immunoblotting as in Fig. 3b setting the amount of unprocessed PARP at 100%. **b**, ES cells were treated with proapoptotic reagents for the indicated periods and the cells with the cytochrome c in the cytosol were quantified by immunofluorescence microscopy. At least 100 cells in more than 3 distinct fields were analyzed. **c**, Drp1$^{-/-}$ MEFs were treated with etoposide for the indicated periods, and the cells were analyzed by immunofluorescence microscopy. The cells with released Smac/Diablo and cytochrome c were counted. At least 100 cells in 3 independent experiments were counted. **d**, The cells obtained in (**c**) were analyzed by SDS-PAGE and subsequent immunoblotting using antibodies against the caspase 3 fragment and Tom40 as a loading control. **e**, MEFs were treated with actinomycin D for the indicated periods and exposure of phosphatidylserine on the outer plasma membrane was measured by flow cytometry after staining the cells with annexin V-FITC. **f** and **g**, Drp1$^{-/-}$ MEFs expressing Tim8-FLAG were treated with actino- mycin D for the indicated periods and the number of cells that contained Tom8a-released but cytochrome c-unreleased mitochondria was counted. Thirty cells each from 3 distinct optical fields were analyzed. Scale bar, 20 μm.

© 2009 Macmillan Publishers Limited. All rights reserved.

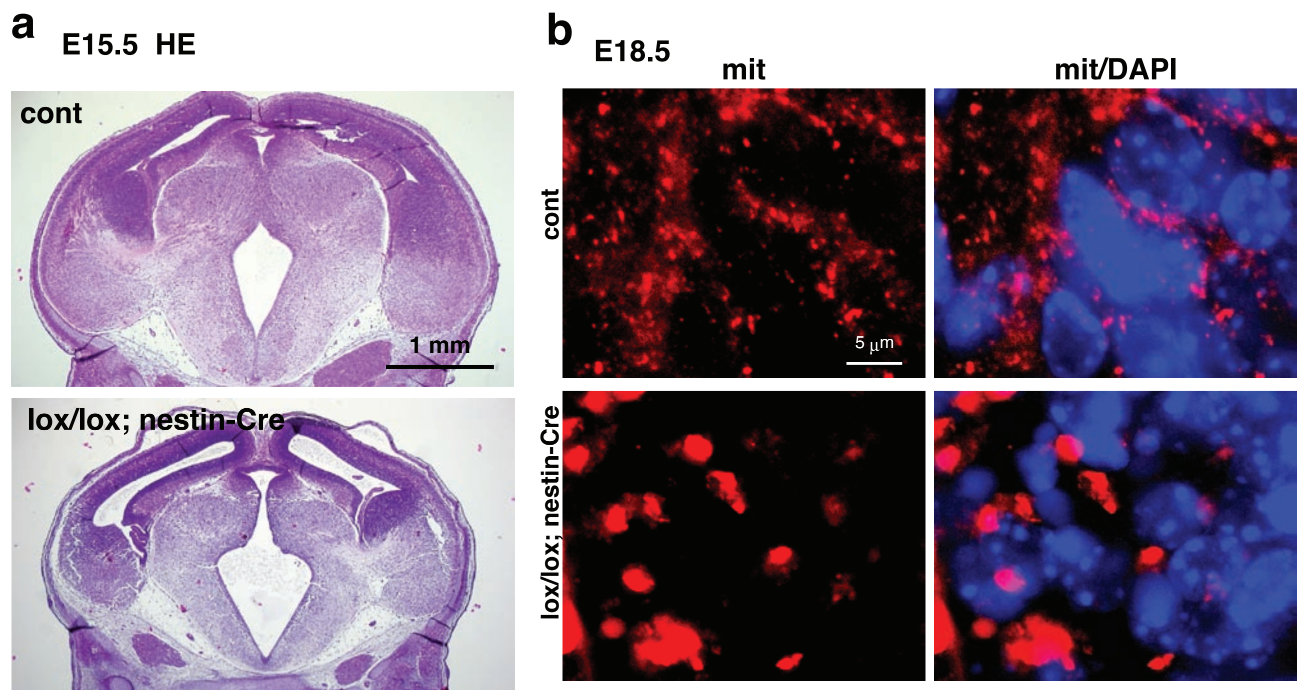

Figure S6 a, Coronal sections of the brain from E15.5 controls or Drp1lox/lox; nestin-Cre mice embryos were HE-stained. **b**, Paraffin-embedded brain sections of E18.5 Drp1lox/lox; nestin-Cre embryos were examined by immunofluorescent microscopy using antibodies against the complex III core 1 protein. Forebrain regions are shown. Clustered mitochondria were observed in the Drp1$^{-/-}$ mouse brain.

© 2009 Macmillan Publishers Limited. All rights reserved.

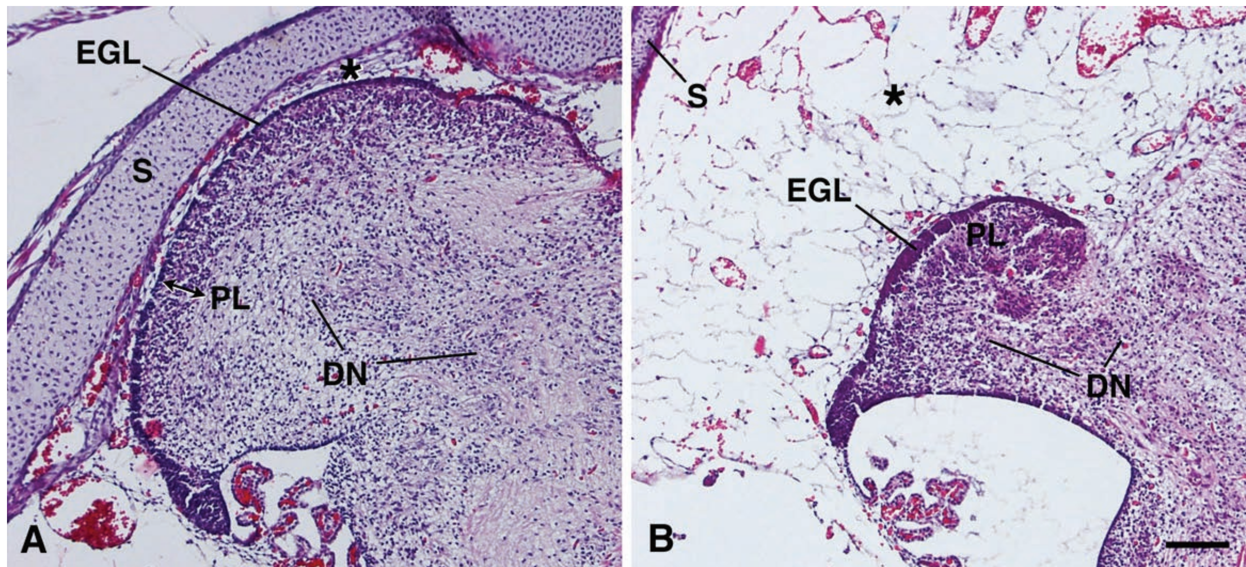

Figure S7 Parasagittal sections of cerebella from E20 control (A) and NS-Drp1$^{-/-}$ (B) mice. Remarkable overall size reduction of the cerebellum as well as the brainstem is noted in NS-Drp1$^{-/-}$ mouse. While the thickness of the forming cerebellar cortex (EGL+PL) and the formation of the DN in the NS-Drp1$^{-/-}$ cerebellum are comparable to those in the control, the white matter of the former shows marked hypoplasia. Note the apparent enlargement of the subdural/subarachnoid space in the posterior fossa in NS-Drp1$^{-/-}$ mouse (asterisk). S; skull, EGL; external granular layer, PL; Purkinje cell layer, DN; dentate nucleus, asterisk: subdural/subarachnoid layer. Bar=100 μm.

© 2009 Macmillan Publishers Limited. All rights reserved.

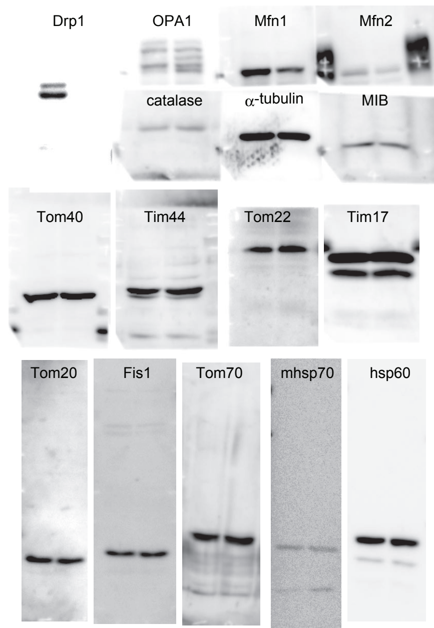

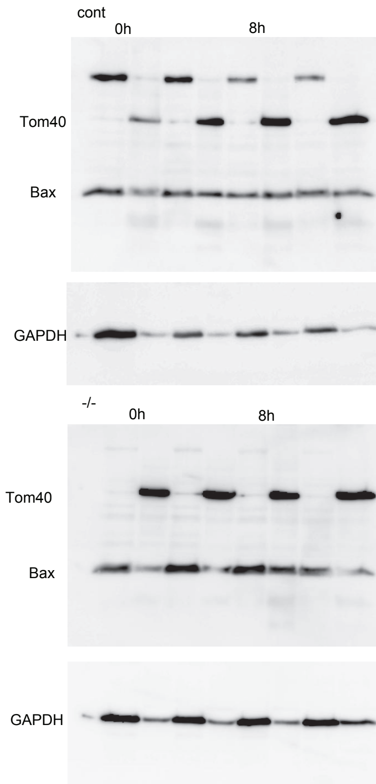

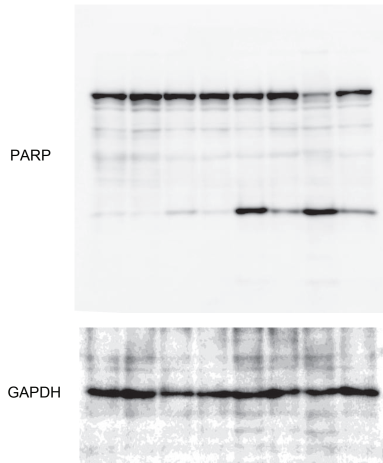

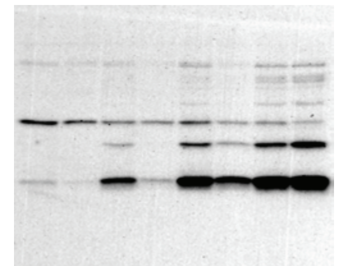

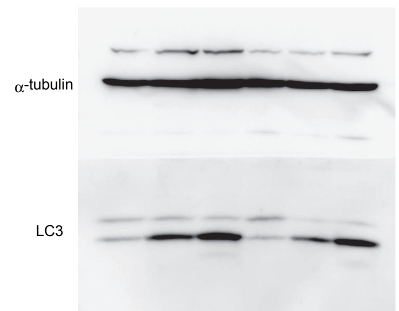

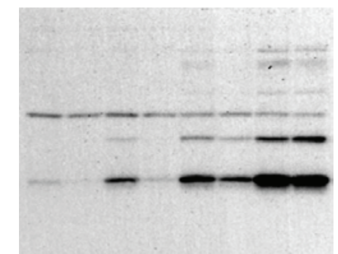

Figure S8 Full scans of the Western blots from the figures.

© 2009 Macmillan Publishers Limited. All rights reserved.